

*J. Synchrotron Rad.* (1999), **6**, 770–772

## Real-space multiple-scattering analysis of Ag $L_1$ - and $L_3$ -edge XANES spectra of $\text{Ag}_2\text{O}$

Ondřej Šipr,<sup>a\*</sup> Francesco Rocca<sup>b</sup> and Giuseppe Dalba<sup>c</sup>

<sup>a</sup>*Institute of Physics, Academy of Sciences of the Czech Republic, Cukrovarnická 10, 162 53 Praha 6, Czech Republic,* <sup>b</sup>*CEFSA-Centro CNR di Fisica degli Stati Aggregati, Povo (Trento), Italy,* and <sup>c</sup>*INFM and Department of Physics, University of Trento, Trento, Italy. E-mail: šipr@fzu.cz*

Real-space multiple-scattering analysis of Ag  $L_1$  and  $L_3$  edge XANES spectra of  $\text{Ag}_2\text{O}$  was performed. The experiment is reproduced with sufficient accuracy provided that the scattering potential is taken from a selfconsistent molecular calculation. A non-selfconsistent potential produces a fairly accurate reproduction of the experiment as well, however, those results are a bit ambiguous to interpret close to the  $L_3$  edge. The  $L_1$  edge spectrum is much less sensitive both to the way of constructing the scattering potential and to presence or absence of the core hole than the  $L_3$  edge. At least fifteen atoms are needed to reproduce the main peaks at the  $L_1$  edge while just three atoms are enough to reproduce the appearance of the dominant structure of the  $L_3$  edge.

**Keywords:**  $\text{Ag}_2\text{O}$ ; real-space multiple-scattering method; selfconsistent potential; core hole effect; silver borate glasses.

### 1. Introduction

X-ray absorption near-edge structure (XANES) spectroscopy can in principle yield both structural and chemical information. The chemical information about  $\text{Ag}_2\text{O}$  is interesting mainly because it has the same structure as its isoelectronic analogue  $\text{Cu}_2\text{O}$ , with obvious links to high temperature superconductors. The structural information may be utilized e.g. in studying the local coordination of silver atoms in fast ion conducting glasses of the type  $\text{AgI-Ag}_2\text{O-B}_2\text{O}_3$ . Czyżyk *et al* (1989) compared Ag  $L$  edge spectra with densities of states (DOS) projected onto the Ag site. Their work dealt mainly with the *chemical* content of XANES.

In this study, we concentrate on the *structural* aspect of XANES spectra of  $\text{Ag}_2\text{O}$ . We calculate Ag  $L_1$  and  $L_3$  edge spectra using the real-space multiple-scattering (RS-MS) method. Results obtained for various scattering potentials are compared. Finally, we study the effect of size of the cluster on particular spectral peaks.

### 2. Methods

The XANES measurements were performed in the transmission mode at the PWA wiggler source in ADONE (Frascati - Italy) (see Czyżyk *et al* (1989) for details). The real-space multiple-scattering calculations were performed using an amended ICXANES code of Vvedensky *et al* (1986). A non-selfconsistent muffin-tin potential was constructed using the prescription of Mattheiss (superposition of potentials of isolated atoms). The effect of the core hole was simulated by putting the core electron of the absorbing Ag atom

into its lowest unoccupied level in the atomic calculation. This is equivalent to the frequently used “Z+1” approximation.

Another muffin-tin potential was obtained from a selfconsistent molecular calculation for a cluster of 27 atoms ( $\text{Ag}_{19}\text{O}_8$ ). Cluster of this size ought to describe bulk properties of crystalline  $\text{Ag}_2\text{O}$  with a sufficient accuracy (Wu *et al* 1993, Soldatov *et al* 1995). The  $X\alpha$  multiple-scattering calculation of molecular orbitals was done using an adapted XASCF program of Cook & Case (1980). The main change in the original XASCF program was necessitated by the fact that managing a cluster as large as 27 atoms required to substitute search for zeros of secular determinant with finding its zero eigenvalues in procedures for finding one-electron energies (Case & Yang 1980). The influence of the core hole was taken into account by keeping one core electron in the valence region while performing a selfconsistent calculation (screened and relaxed model).

### 3. Results and discussion

In Fig. 1 and Fig. 2, we present experimental  $L_1$  and  $L_3$  spectra together with theoretical curves obtained for both selfconsistent and non-selfconsistent potentials, either with or without a core hole. By calculating the  $2p \rightarrow s$  and  $2p \rightarrow d$  matrix elements, we found that in the  $L_3$  spectrum, the  $d$  states dominate over  $s$  states by an order of magnitude. Hence,  $L_{2,3}$  spectra of  $\text{Ag}_2\text{O}$  reflect nearly pure  $d$  states DOS.

Solid thick lines in Fig. 1 and Fig. 2 represent theoretical spectra convoluted with lorentzian curves to account for finite core hole lifetimes, as compiled by Al Shamma *et al* (1992). Original “raw” theoretical data are shown with thin dashed lines as well. Those curves include also occupied states lying just above the muffin-tin zero but below the chemical potential.

The chemical potential — the threshold of the absorption edge — was chosen by convenience so that it coincides with a dip of the raw  $L_3$  spectrum (mimicking thus the semiconducting gap). As the chemical potential can be estimated only with a precision of few electronvolts without performing the band-structure calculation, such a fitting is justified within the current computational scheme (Mustre de Leon *et al* 1991, Ankudinov *et al* 1998).

At the Ag  $L_1$  edge (Fig. 1), there are no really striking differences between results obtained for a selfconsistent and for a non-selfconsistent potential. The energy separation between the peaks marked A and B in the plot is smaller for the selfconsistent potential than for the non-selfconsistent one — the experimental distance falls in the middle. The non-selfconsistent potential provides lower intensity of the peak B than of the C peak, contrary to the experiment. Using selfconsistent potential corrects for this deficiency. The effect of the core hole is almost negligible at the  $L_1$  edge.

The Ag  $L_3$  edge (Fig. 2) offers more details to compare. The selfconsistent potential performs significantly better than the non-selfconsistent one. This applies especially to peaks B and C: Although these two peaks can be recognized in the spectra generated by the non-selfconsistent potential, their positions and relative intensities are not sufficiently accurate to allow for an unambiguous identification. Even in the case of the selfconsistent potential, the peak B is too small and remains barely visible after the smearing (similarly as peak A at the  $L_1$  edge — cf. Fig. 1).

The core hole changes the height of the white line A at the  $L_3$  edge dramatically while it leaves the  $L_1$  spectrum intact. The fact that core hole effects  $d$  states much more than  $p$  states was observed also for  $\text{Cu}_2\text{O}$  (Grioni *et al* 1992) and for transition metals (Tamura *et al* 1995). In our case the core hole *decreases* the  $L_3$

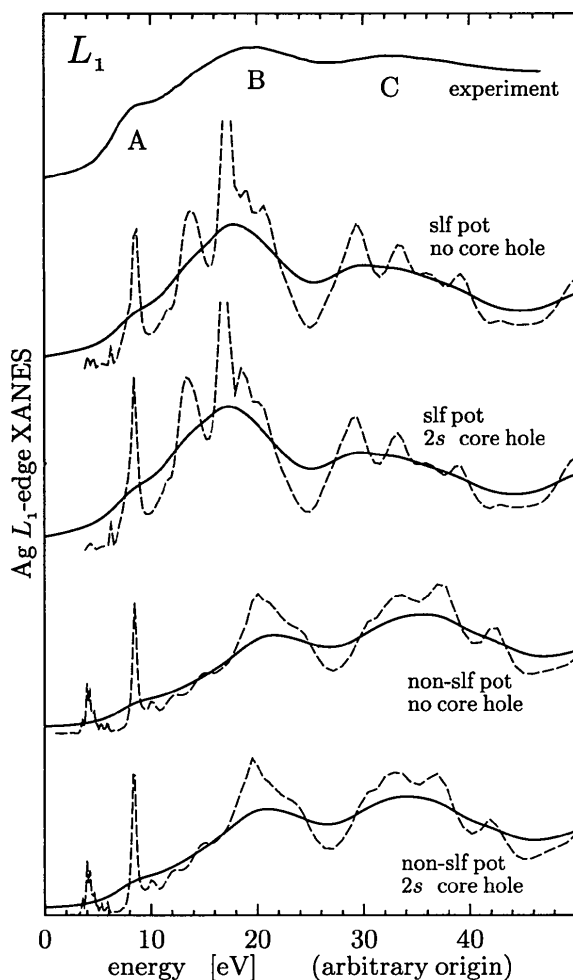


**Figure 1**

Experimental and theoretical XANES spectra of  $\text{Ag}_2\text{O}$  at the  $\text{Ag } L_1$  edge. The theoretical spectra are presented for four different types of scattering potential (a non-selfconsistent Mattheiss potential and a self-consistent potential of a 27-atoms molecular cluster, both with and without a core hole). Thick solid lines are theoretical results smeared by lorentzian curve of FWHM equal to core hole lifetime broadening (4.88 eV), thin dashed lines represent raw calculated spectra.

white line. For a selfconsistent potential, this improves the agreement with the experiment, while for a non-selfconsistent potential the decrease in white line intensity is too large. We can recall that in semiconducting  $\text{Cu}_2\text{O}$  the inclusion of the core hole increases the white line intensity (Groni *et al* 1992), contrary to transition metals where it decreases the  $L_3$  white line (Tamura *et al* 1995). Hence one could suggest that the fully relaxed and screened model applied in this study overestimates the screening in the case of a non-selfconsistent potential, being suitable rather to metals than to semiconductors. On the other hand, unscreened and/or unrelaxed non-selfconsistent core hole potentials performed badly at  $K$  edge spectra of chalcogenide semiconductors (Šipr *et al* 1997). It seems therefore that simple ways of incorporating a core hole may not work universally in cases when large core hole effects are expected.

The dependence of the calculated XANES spectra on the increasing size of the cluster is shown in Fig. 3 for the  $L_1$  edge and in Fig. 4 for the  $L_3$  edge. Information of this kind is valuable for

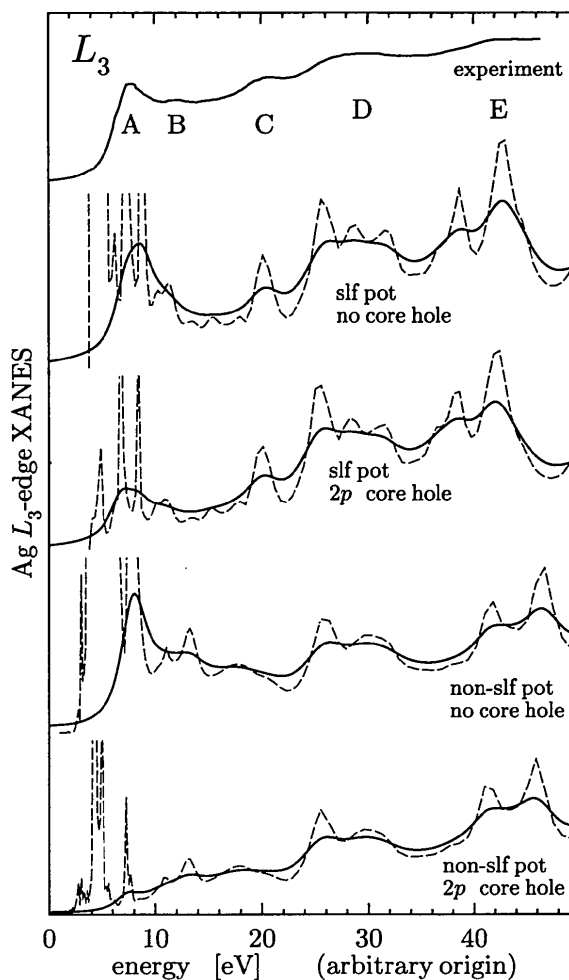


**Figure 2**

Experimental and theoretical XANES spectra of  $\text{Ag}_2\text{O}$  at the  $\text{Ag } L_3$  edge. The theoretical spectra are presented for four different types of scattering potential (a non-selfconsistent Mattheiss potential and a self-consistent potential of a 27-atoms molecular cluster, both with and without a core hole). Thick solid lines are theoretical results smeared by lorentzian curve of FWHM equal to core hole lifetime broadening (2.40 eV), thin dashed lines represent raw calculated spectra.

possible applications of XANES in structural analysis. In particular it was found by Dalba *et al* (1986) that  $\text{Ag } L_1$  spectra of silver borate glasses  $\text{Ag}_2\text{O} \cdot n\text{B}_2\text{O}_3$  differ substantially from  $L_1$  spectrum of crystalline  $\text{Ag}_2\text{O}$ , while the  $L_3$  edges of  $\text{Ag}_2\text{O} \cdot n\text{B}_2\text{O}_3$  and of  $\text{Ag}_2\text{O}$  are quite similar to each other (apart from an obvious smearing of details). Fig. 4 reveals that the basic shape of the  $L_3$  edge of  $\text{Ag}_2\text{O}$  is determined just by the central Ag atom and its two nearest oxygens. On the other hand, the underlying structure of the  $L_1$  edge gets revealed only if at least 15 atoms are taken into account (see Fig. 3). Hence on the basis of this comparative XANES analysis of  $\text{Ag}_2\text{O}$ , we can suggest that in silver borate glasses only the first coordination shell of Ag is more or less the same as in crystalline  $\text{Ag}_2\text{O}$ , while the more distant coordinations differ significantly.

This research was carried out within the framework of the Agreement for scientific cooperation between the National Research Council of Italy (CNR) and the Academy of Sciences of the Czech Republic (AV ČR). One of the authors (O. Š.) gratefully ac-

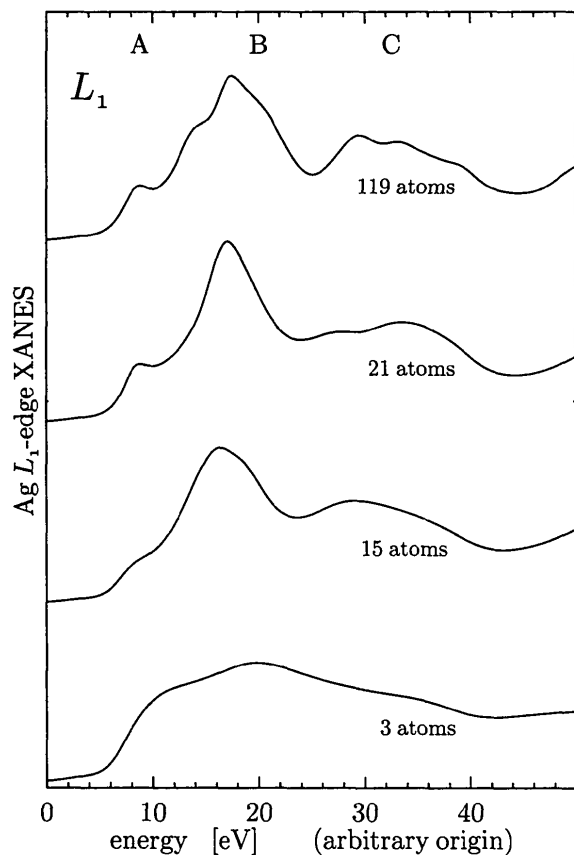


**Figure 3**

Theoretical Ag  $L_1$  edge spectra of  $\text{Ag}_2\text{O}$  for increasing cluster sizes. A selfconsistent potential without a core hole was used. To preserve more details of the calculated spectra, each curve was smeared by a lorentzian of FWHM equal only to a half of the respective core hole lifetime broadening, i.e. 2.44 eV .

knowledges support by the grant 202/97/0566 of the Grant Agency of the Czech Republic.

### References

- Al Shamma, F., Abbate, M. & Fuggle, J. C. (1992). Unoccupied Electronic States, edited by J. C. Fuggle & J. E. Inglesfield, pp. 347–351. Berlin: Springer.
- Ankudinov, A. L., Conradson, S. D., Mustre de Leon, J. & Rehr, J. J. (1998). *Phys. Rev. B* **57**, 7518–7525.
- Case, D. A. & Yang, C. Y. (1980). *Int. J. Quantum Chem.* **18**, 1091–1099.
- Cook, M. & Case, D. A. (1980). Computer code XASCF. Quantum Chemistry Program Exchange, Indiana University, Bloomington, Indiana.
- Czyżyk, M. T., de Groot, R. A., Dalba, G., Fornasini, P., Kisiel, A., Rocca, F. & Burattini, E. (1989). *Phys. Rev. B* **39**, 9831–9838.

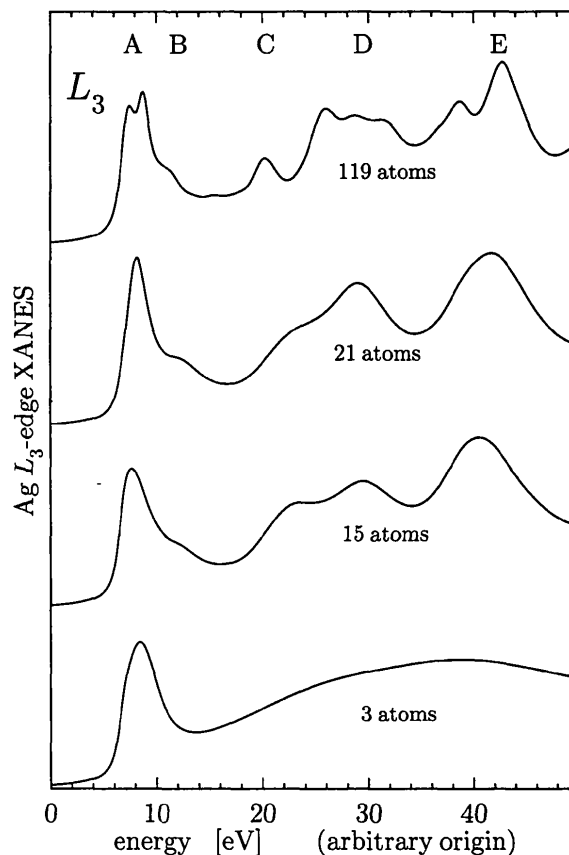


**Figure 4**

Theoretical Ag  $L_3$  edge spectra of  $\text{Ag}_2\text{O}$  for increasing cluster sizes. A selfconsistent potential without a core hole was used. To preserve more details of the calculated spectra, each curve was smeared by a lorentzian of FWHM equal only to a half of the respective core hole lifetime broadening, i.e. 1.20 eV .

- Dalba, G., Fornasini, P., Rocca, F. & Burattini, E. (1986). *J. Phys. (Paris)* **47**, C8-749–C8-752.
- Griani, M., van Acker, J. F., Czyżyk, M. T. & Fuggle, J. C. (1992). *Phys. Rev. B* **45**, 3309–3318.
- Mustre de Leon, J., Rehr, J. J., Zabinsky, S. I. & Albers, R. C. (1991). *Phys. Rev. B* **44**, 4146–4156.
- Sipr, O., Machek, P., Šimůnek, A., Vackář, J. & Horák, J. (1997). *Phys. Rev. B* **56**, 13151–13161.
- Soldatov, A. V., Ivanchenko, T. S., Kovtun, A. P., Della Longa, S. & Bianconi, A. (1995). *Phys. Rev. B* **52**, 11757–11762.
- Tamura, E., van Ek, J., Fröba, M. & Wong, J. (1995). *Phys. Rev. Lett.* **74**, 4899–4902.
- Vvedensky, D. D., Saldin, D. K. & Pendry, J. B. (1986). *Comput. Phys. Commun.* **40**, 421–440.
- Wu, Z. Y., Benfatto, M. & Natoli, C. R. (1993). *Solid State Commun.* **87**, 475–480.

(Received 10 August 1998; accepted 21 December 1998)